Solving One-Dimensional Moving-Boundary Problems with Meshless Method

4 authors:

Leopold Vrankar
Ministry of Infrastructure, Ljubljana, Slovenia
16 PUBLICATIONS **62** CITATIONS

Edward Kansa
Convergent Solutions
144 PUBLICATIONS **7,611** CITATIONS

Goran Turk
University of Ljubljana
115 PUBLICATIONS **1,643** CITATIONS

Franc Runovc
University of Ljubljana
33 PUBLICATIONS **256** CITATIONS

Some of the authors of this publication are also working on these related projects:

Project   seperate View project

Project   funding terminated View project

Solving one-dimensional moving-boundary problems with meshless method

Leopold Vrankar

Slovenian Nuclear Safety Administration
Železna cesta 16, 1001 Ljubljana, Slovenia

Edward J. Kansa

Department of Mechanical and Aeronautical Engineering, University of California,
USA

Goran Turk

University of Ljubljana, Faculty of Civil and Geodetic Engineering
Jamova cesta 2, 1000 Ljubljana, Slovenia

Franc Runovc

University of Ljubljana, Faculty of Natural Sciences and Engineering
Aškerčeva cesta 12, 1000 Ljubljana, Slovenia

Abstract

Many physical processes involve heat conduction and materials undergoing a change of phase. Examples include the safety studies of nuclear reactors, casting of metals, semiconductor manufacturing, geophysics and industrial applications involving metals, oil, and plastics. Due to their wide range of applications the phase change problems have drawn considerable attention of mathematicians, engineers and scientists. These problems are often called Stefan's or moving boundary value problems. One common feature of phase change problems is that the location of the solid-liquid or solid-solid interface is not known a priori and must be determined during the course of analysis. Mathematically, the interface motion is expressed implicitly in an equation for the conservation of thermal energy at the interface (Stefan's conditions). This introduces a non-linear character to the system which treats each problem somewhat uniquely. The exact solution of phase change problems is limited exclusively to the cases in which e.g. the heat transfer regions are infinite or semi-infinite one dimensional-spaces. Therefore, solution is obtained either by approximate analytical solution or by numerical methods. Finite-difference methods and finite-element techniques have been used extensively for numerical solutions of moving boundary problems. Recenty, the numerical methods have focused on the idea of using a meshless methodology for the numerical solution of

partial differential equations based on radial basis functions. One of the common characteristics of all meshless methods is their ability to construct functional approximation or interpolation entirely based on the information given at a set of scattered nodes. In our case we will study solid state phase transformation problem in binary metallic alloys. The numerical solutions will be compared with analytical solutions. Actually, in our work we will examine usefulness of radial basis functions for one-dimensional Stefan's problems. The position of the moving boundary will be simulated by moving grid method.

Key words: Moving-boundary problems, Meshless method, Radial basis functions, Stefan's problems, Moving grid method

---

1 Introduction

A large number of important physical processes involve heat conduction and materials undergoing a change of phase. Examples include nuclear reactors, casting of metals, semiconductor manufacturing, geophysics, and industrial applications involving metals, oil, and plastics. These problems often are called Stefan's or moving boundary value problems. Analytical solutions are only available for a limited number of model examples and hence the solution of most practical cases requires the use of numerical techniques. The exact solution of phase change problems is limited exclusively to the cases in which e.g. the heat transfer regions are infinite or semi-infinite one dimensional-spaces.

Several numerical methods have been developed to solve various Stefan's problems. Crank [1] provides a good introduction to the Stefan's problems and presents an elaborate collection of numerical methods for these problems. According to Crank the numerical methods for moving boundary problems can be classified in three categories: front-tracking methods, front-capturing methods and hybrid methods. We follow front-tracking methods (moving grid method) which use an explicit representation of the interface, given by a set of points lying on the interface location, which must be updated at each time step.

The meshless method has been widely investigated in the past and emerged as a new category of computational methods. One of its advantages is that no mesh generation is required to solve differential equations numerically. It is well known that in the traditional numerical methods, such as finite element methods, finite difference methods, boundary element methods, it is usually difficult and takes considerable effort to generate proper meshes for computational purposes. This is especially true for three–dimensional problems with complicated geometry in engineering applications.

Heat treatment of metals is often used to optimize mechanical properties. Dur-

ing heat treatment, the metallurgical state of the alloy changes. This change can involve the phase present at a given location or the morphology of the various phases. Whereas equilibrium phases can be predicted quite accuratly from thermodynamic models, there are no general models for microstructural changes nor for the kinetics of these changes. One of these processes, which is both of large industrial and scientific interest and amenable to modeling, is the dissolution of the second–phase particles in a matrix with a uniform initial composition.

In our case we will study solid state phase transformation problem in binary metallic alloys. The numerical solutions will be compared with analytical solutions. Actually, in our work we will examine usefulness of radial basis functions for one–dimensional Stefan's problems. The position of the moving boundary will be simulated by moving grid method.

2   The Meshless Method

The meshless method is currently at the stage of development. Various approaches and computational procedures have been proposed in the literature. Not every method that is claimed to be meshless is really meshless. The true meshless method must provides a computational procedure without relating to any mesh point connectivity.

Three different approaches to develop meshless methods have been successfully proposed. The first one is based on the spirit of the finite element method and employs Petrov–Galerkin weak formulation. Detailed theories and formulation can be found in the book by Atluri and Shen [2].

The second approach is of boundary element type. It attempted to discretize boundary integral formulation without employing a mesh. Grid points in this approach are all on the boundaries. Several procedures [3] have been proposed with different discretization concepts.

The third approach employs radial basis functions (RBFs). The base of this approach is its employment of high-order interpolating functions to approximate solutions of differential equations. All RBFs possess the property that their values are determined only by distance and have nothing to do with directions. Kansa [4]–[5] introduced multiquadric functions to solve hyperbolic, parabolic and elliptic differential equations with collocation methods. This method is an asymmetric collocation set–up in which boundary conditions are treated separately from the interior problem. He found that they had quite good convergence properties and achieved outstanding computational efficiency. One of the most powerful RBF method is based on multiquadric basis functions

(MQ), first used by R. L. Hardy [6]. It is important to mentioned that the MQ was till now efficiently used in transport modelling [7]–[8]. In our case we focused on using RBFs with collocation methods.

3 Radial Basis Function Methods

Radial basis function methods have been praised for their simplicity and ease of implementation in multivariate scattered data approximation [9], and they are becoming a viable choice as a method for the numerical solution of partial differential equations [4]–[5]. Compared to low–order methods such as finite differences, finite volumes and finite elements, RBF–based methods offer numerous advantages, such as no need for a mesh or triangulation, simple implementation and dimensional indenpendence, and no staircasing or polygonization for boundaries.

A radial basis function is a function $\phi_j(\mathbf{x}) = \phi(\|\mathbf{x} - \mathbf{x}_j\|)$, which depends only on the distance between $\mathbf{x} \in \mathbf{R^d}$ and a fixed point $\mathbf{x}_j \in \mathbf{R^d}$. Here, ϕ is continuous and bounded on any bounded sub-domain $\Omega \subseteq \mathbf{R^d}$. Let r denote by the Euclidean distance between any pair of points in the domain Ω.

The commonly used radial basis functions are:

$$
\begin{aligned}
&\phi(r) = r, &&\text{linear,} \\
&\phi(r) = r^3, &&\text{cubic,} \\
&\phi(r) = r^2 \log r, &&\text{thin-plate spline,} \\
&\phi(r) = e^{-cr^2}, &&\text{Gaussian,} \\
&\phi(r) = (r^2 + c^2)^{\frac{1}{2}}, &&\text{multiquadric,} \\
&\phi(r) = (r^2 + c^2)^{-\frac{1}{2}}, &&\text{inverse multiquadric.}
\end{aligned}
$$

To introduce RBF collocation methods, we consider a PDE in the form of

$$L\,u = f(\mathbf{x}) \quad \text{in} \quad \Omega \subset \mathbf{R^d}, \tag{1}$$

$$B\,u = g(\mathbf{x}) \quad \text{on} \quad \partial\Omega, \tag{2}$$

where u is concentration, $\mathbf{d}$ is the dimension, $\partial\Omega$ denotes the boundary of the domain Ω, L is the differential operator on the interior, and B is an operator that specifies the boundary conditions of the Dirichlet, Neumann or mixed

type. Both, f and g, are given functions mapping $\mathbf{R^d} \to \mathbf{R}$.

The solution, u, to the PDE is approximated by linear combination of RBFs and polynomials:

$$u \approx U(\mathbf{x}) = \sum_{j=1}^{N} \alpha_j \phi_j(\mathbf{x}) + \sum_{l=1}^{M} \gamma_l v_l(\mathbf{x}), \tag{3}$$

where $\phi_j(\mathbf{x}) = \phi(\|\mathbf{x} - \mathbf{x}_j\|)$, and ϕ can be any radial basis function from the list, $v_1, \ldots, v_M \in \Pi_m^d$ is a polynomial of degree m or less, $M := \binom{m-1+d}{d}$ [10] and $\| \cdot \|$ indicates the Euclidean norm. Let $\{(\mathbf{x}_j)\}_{j=1}^{N}$ be the $N = N_I + N_B$ collocation points in $\Omega \cup \partial\Omega$. We assume the collocation points are arranged in such a way that the first N_I points are in Ω, whereas the last N_B points are on $\partial\Omega$. To solve for the $N + M$ unknown coefficients, $N + M$ linearly independent equations are needed. By choosing N distinct collocation points $X_I = \{\mathbf{x}_1, \ldots, \mathbf{x}_{N_I}\} \subset \Omega$ and $X_B = \{\mathbf{x}_{N_I+1}, \ldots, \mathbf{x}_N\} \subset \partial\Omega$ and ensuring that $U(\mathbf{x})$ satisfies (1) and (2) at the collocation points results in a good approximation of the solution u. The first N equations are given by

$$\sum_{j=1}^{N} \alpha_j \, L \, \phi_j(\mathbf{x}_i) + \sum_{l=1}^{M} \gamma_l \, L \, v_l(\mathbf{x}_i) = f(\mathbf{x}_i) \quad \text{for} \quad i = 1, \ldots, N_I$$

$$\sum_{j=1}^{N} \alpha_j \, B \, \phi_j(\mathbf{x}_i) + \sum_{l=1}^{M} \gamma_l \, B \, v_l(\mathbf{x}_i) = g(\mathbf{x}_i) \quad \text{for} \quad i = N_I + 1, \ldots, N \tag{4}$$

The last M equations could be obtained by imposing some extra condition on $v(\cdot)$:

$$\sum_{j=1}^{N} \alpha_j v_k(\mathbf{x}_j) = 0, \quad k = 1, \ldots, M. \tag{5}$$

This leads to the equivalent matrix form: $\mathbf{A}\mathbf{x} = \mathbf{b}$ or

$$\begin{bmatrix} \mathbf{W_L} & \mathbf{v_L} \\ \mathbf{W_B} & \mathbf{v_B} \\ \mathbf{v^T} & \mathbf{0} \end{bmatrix} \begin{bmatrix} \boldsymbol{\alpha} \\ \boldsymbol{\gamma} \end{bmatrix} = \begin{bmatrix} \mathbf{f} \\ \mathbf{g} \\ \mathbf{0} \end{bmatrix}, \tag{6}$$

where

$$\mathbf{W_L} = L \, \phi_j(\mathbf{x}_i), \quad \mathbf{x}_i \in X_I \tag{7}$$

$$\mathbf{v_L} = L\, v_l(\mathbf{x}_i), \quad \mathbf{x}_i \in X_I \tag{8}$$

$$\mathbf{W_B} = B\, \phi_j(\mathbf{x}_i), \quad \mathbf{x}_i \in X_B \tag{9}$$

$$\mathbf{v_B} = B\, v_l(\mathbf{x}_i), \quad \mathbf{x}_i \in X_B \tag{10}$$

The choice of basis function is another flexible features of RBF methods. RBFs can be globally supported, infinitely differentiable, and contain a free parameter, c, called the *shape parameter*. This leads to a full coefficient matrix or a dense interpolation matrix. In addition, in solving simultaneous algebraic equations, they easily result in poor conditioned coefficient matrices. Global, infinitely differentiable RBFs typically interpolate smooth data with spectral accuracy [9].

The shape parameter affects both the accuracy of the approximation and the conditioning of the interpolation matrix. In general, for a fixed number of centers N, smaller shape parameters produce the more accurate approximations, but also are associated with a poorly conditioned matrix. The condition number also grows with N for fixed values of the shape parameter c. In practice, the shape parameter must be adjusted with the number of centers in order to produce an interpolation matrix which is well conditioned enough to be inverted in finite precision arithemetic. Many researchers (e.g. [11]–[12]) have attempted to develop algorithms for selecting optimal values of the shape parameter c. The optimal shape parameter c is still an open question. In our case we used an iterative mode by monitoring the spatial distribution of the residual errors in Ω and $\partial\Omega$ as a function of c. The iterations are terminated when errors are smaller then a specified bound. This map is then used to guide the search of the optimal shape parameter c that the best approximate the solution. In our study we used in general multiquadric (MQ) RBF. The generalized form of the MQ basis function is $\phi_j(\mathbf{x}) = [(\mathbf{x} - \mathbf{x}_i)^2 + c_i^2]^{\beta}$, where $\mathbf{x}, \mathbf{x}_i \in \mathbf{R^d}$, and β is a non integer $\geq -1/2$.

Our intent is also to use anti–differentiation upon gradients of dependent variables. Mai–Duy and Tran–Cong [15] obtained very impressive computational results with singly or doubly integrated MQ RBFs.

The methodology of the integral formulation is similar, except that we integrate the MQ:

$$\psi_j(x) = \sqrt{(x - x_j)^2 + c^2} \tag{11}$$

6

with respect to x twice to obtain the new basis functions:

$$\Phi_j(x) = \frac{1}{6}\Big((x - x_j)^2 - 2c^2\Big)\psi_j(x) + \frac{1}{2}(x - x_j)\Big(c^2\Big)\ln\Big((x - x_j) + \psi_j(x)\Big) \tag{12}$$

whose derivatives are

$$\frac{\partial \Phi_j(x)}{\partial x} = \frac{1}{2}(x - x_j)\psi_j(x) + \frac{1}{2}\Big(c^2\Big)\ln\Big((x - x_j) + \psi_j(x)\Big), \tag{13}$$

$$\frac{\partial^2 \Phi_j(x)}{\partial x^2} = \psi_j(x). \tag{14}$$

The expansion of the unknown function is now of the form:

$$u(\mathbf{x}) = \sum_{j=1}^{N} \alpha_j \Phi_j(\mathbf{x}) + \sum_{l=1}^{M} \gamma_l v_l(\mathbf{x}). \tag{15}$$

4   The problem

4.1   The physical model

In this study we consider classical Stefan's problem: the solid state phase transformation problem in binary metallic alloys which is described in [13]. In that problem a volume of constant composition is surrounded by a diffusive phase. In the interface between the particle and the diffusive phase a constant concentration is assumed, and the gradient of the concentration causes the movement of the interface. This problem is also called solid–solid transformation.

4.2   The mathematical model

We consider the domain Ω containing a diffusive phase Ω_{dp} and the part where the material characteristic Ω_{part} remain of constant composition c^{part}. The particle dissolves due to Fickian diffusion in the diffusive phase. The concentration at the interface Γ, separating Ω_{part} and Ω_{dp}, is assumed to be given by the constant value c^{sol}. The concentration gradient on the side of Ω_{dp} at Γ causes its displacement. The governing equations and boundary conditions of this problem are:

$$\frac{\partial u}{\partial t}(\mathbf{x}, t) = D\Delta u(\mathbf{x}, t), \quad \mathbf{x} \in \Omega_{dp}(t),\ t > 0, \tag{16}$$

$$u(\mathbf{x}, t) = u^{part}, \quad \mathbf{x} \in \Omega_{part}(t),\ t \geq 0, \tag{17}$$

$$u(\mathbf{x}, t) = u^{sol}, \quad \mathbf{x} \in \Gamma(t),\ t \geq 0, \tag{18}$$

$$(u^{part} - u^{sol})v_n(\mathbf{x}, t) = D\frac{\partial u}{\partial \mathbf{n}}(\mathbf{x}, t), \quad \mathbf{x} \in \Gamma(t),\ t > 0, \tag{19}$$

where $\mathbf{x}$ is coordinate vector of a point in Ω, D means the diffusivity constant, $\mathbf{n}$ is the unit normal vector on the interface pointing outward with respect to $\Omega_{part}(t)$ and v_n is the normal component of the velocity of the interface. The initial concentration $u(\mathbf{x}, 0)$ inside the diffusive phase is given. We assume no flux of the concentration through the boundary:

$$\frac{\partial u}{\partial \mathbf{n}}(\mathbf{x}, t) = 0, \quad \mathbf{x} \in \partial\Omega_{dp}(t)\backslash\Gamma(t),\ t > 0, \tag{20}$$

hence mass is conserved.

5   The numerical solution methods

In our model the motion of the interface is determined by the gradient of concentration, which can be computed from the solution of the diffusion equation. Our interest is to give an accurate discretization of the moving boundary conditions. Here we present an interpolative moving grid method, in which the grid is computed for each time step and the solution is interpolated from the old grid to the new. The equations are solved with collocation methods using RBFs. A characteristic feature of a front–tracking method is that the interface positions are nodal points in every time–step. Therefore, the position of the grid points depend on time. An outline of the algorithm is:

- Compute the concentrations profiles solving equations (16), (17), (18) and (20).
- Predict the position of boundary s_1 at the new time–step: $s_1(t + \Delta t)$ using boundary condition (19).
- Once the boundary is moved, the concentration u can be computed in the new region using Eq. (16). The solution is interpolated from the old grid to the new.

6 Analytical solutions

In numerical experiments we will compare our numerical solutions with the analytical solutions that exist for the problem presented above. These solutions are expressed as functions of $\frac{x-s_0}{\sqrt{t}}$ as proved in [14], and the domain $\Omega = [0, l]$ has to be infinite or semi–infinite. The interface position is given by $s(t) = s_0 + 2\alpha\sqrt{t}$, where the constant α is obtained by solving the following equation:

$$\alpha = \frac{u^0 - u^{sol}}{u^{part} - u^{sol}} \sqrt{\frac{D}{\pi}} \frac{\exp(-\frac{\alpha^2}{D})}{\operatorname{erfc}(\frac{\alpha}{\sqrt{D}})}. \tag{21}$$

When α is known, the concentration is given by

$$u(x, t) = \begin{cases} u^{part} & \text{if } x < s(t), \\ u^0 + \frac{(u^{sol} - u^0)\operatorname{erfc}(\frac{x-s_0}{2\sqrt{Dt}})}{\operatorname{erfc}(\frac{\alpha}{\sqrt{D}})}, & \text{if } x \geq s(t), \end{cases}$$

where u^{part} is the concentration inside the particle, u^{sol} is the concentration on the interface and u^0 is the initial concentration of the diffusive phase. s_0 is the initial position of the interface.

We assume a piecewise initial concentrations as follows:

$$u(x, 0) = \begin{cases} u^{part} & \text{if } x \in \Omega_{part} = [0, s_0), \\ u^{sol} & \text{if } x = s_0, \\ u^0 & \text{if } x \in \Omega_{db} = (s_0, l). \end{cases}$$

7 Numerical examples

For the simulations we used data from [13]: the concentration inside the part where the material characteristics remain constant $u^{part} = 0.53$, the concentration on the interface $u^{sol} = 0$, the initial concentration of the diffusive phase $u^0 = 0.1$, the diffusivity constant $D = 1$, the domain length $l = 1$ and the initial position of the interface $s_0 = 0.2$.

Let N be the total number of grid intervals, r of those lie inside constant composition and $N - r$ lie inside the diffusive phase. The grid is uniform in

each phase and the interface is always located in the rth node. Due to the movement of the interface, the grid is adapted at each time step.

7.1   MQ, $\beta = 0.5$

In numerical experiments we will also include MQ exponent, β as additional parameter to be optimized. First, the MQ exponent, β had the value 0.5. In figure 1 the movement of the interface positions calculated with MQ exponent, $\beta = 0.5$ is presented. On the upper side of the figure 1 we show the results obtained by shape parameter c based on residual error calculated at collocation points, and on the lower side of the figure 1 we show the results obtained by shape parameter c based on residual error calculated at other points (those lie between collocation points). During the time simulation steps the shape parameter c had values about 0.01. The tolerance for residual error, ϵ was between $1.e - 5$ and $1.e - 15$.
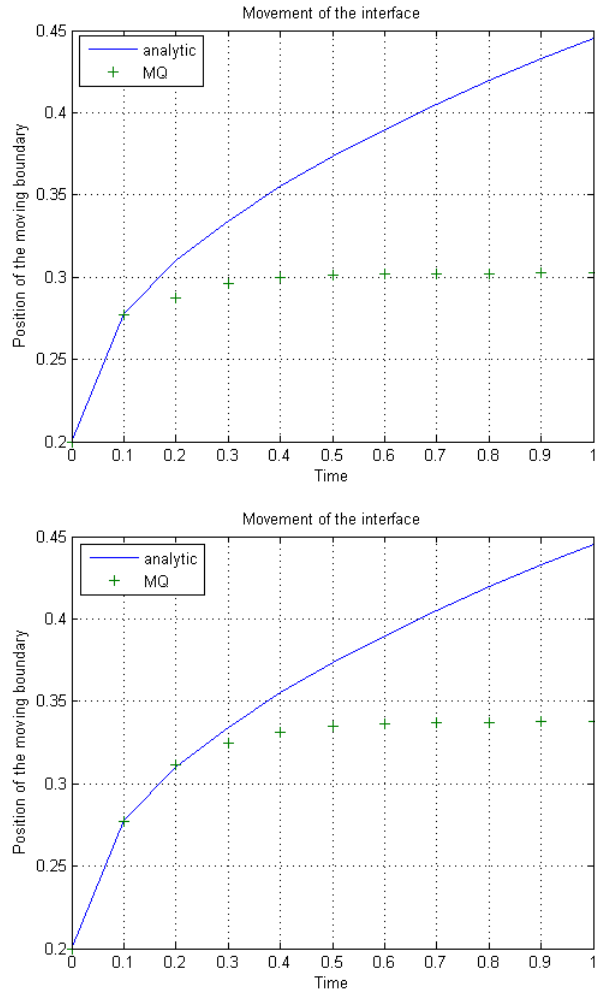

Figure 1: Interface position vs. time simulated with MQ ($\beta = 0.5$)

Second, the MQ exponent parameter, β had the value 1.5. In figure 2 the movement of the interface positions is shown. On the upper side of the figure 2 we show the results obtained by shape parameter c based on residual error calculated at collocation points, and on the lower side of the figure 2 we show the results obtained by shape parameter c based on residual error calculated at other points. During the time simulation steps the shape parameter c had values between 0.01 and 0.09. In the case of the collocation points the tolerance for residual error was $\epsilon = 1.81e - 16$. But in the case of other points the tolerance for residual error was $\epsilon = 0.4$.
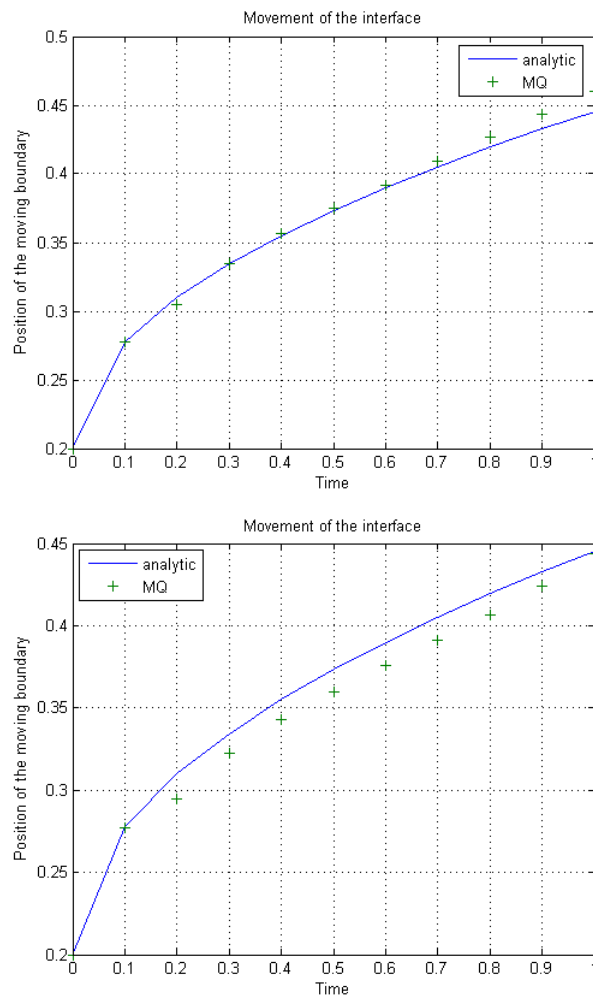

Figure 2: Interface position vs. time simulated with MQ ($\beta = 1.5$)

The movement of the interface where the residual error was determined at interior points is presented in figure 3.
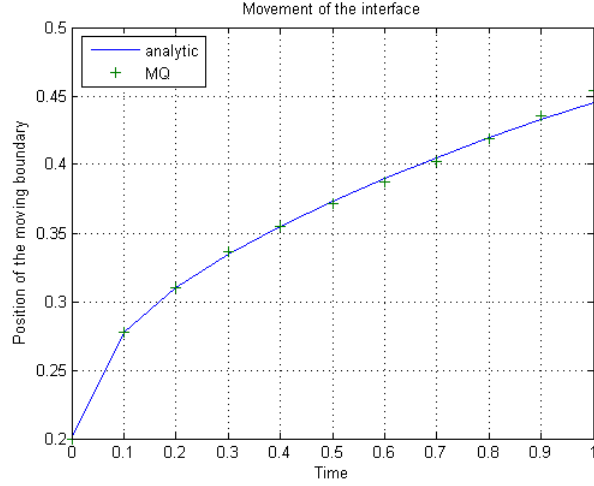
Figure 3: Interface position vs. time simulated with MQ ($\beta = 1.5$)–residual errors determined at interior points

7.3 Integral MQ scheme

In the last cases we present a collocation method based on multiquadric functions with integral formulation for calculation of the movement of the interface positions. The movement of the interface calculated by integral MQ scheme is shown in figure 4. The shape parameter c was obtained by residual error procedure.
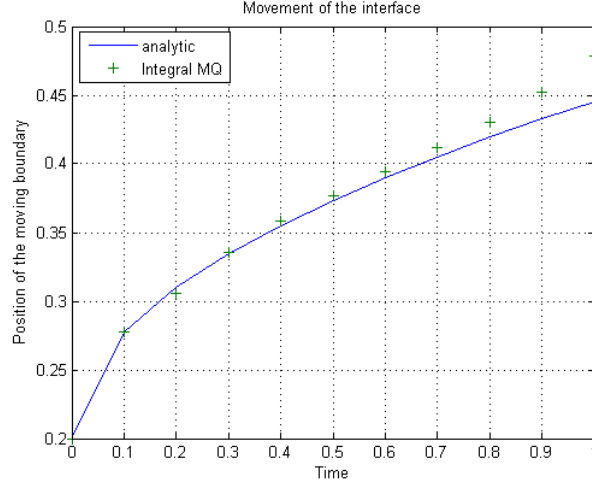

Figure 4: Interface position vs. time simulated with integral MQ scheme

8 Discussion

Comparison of positions of the moving boundary calculated with MQ ($\beta = 0.5$) and MQ ($\beta = 1.5$) (Figure 1 and Figure 2) shows that MQ ($\beta = 1.5$)

determines the position of the interfaces much more accurately than MQ ($\beta = 0.5$). The simulations have also show that the value of the shape parameter c which was computed by residual error procedure was in range between 0.01–0.09. This confirm the fact that for a fixed number of centers N, smaller shape parameters produce the more accurate approximations. The results have shown that β should be greater than 0.5 if we want to get reasonable results. The shape parameter c determined at collocation points better fulfill equation than the shape parameter c determined at the other points. Probably reasons for bad results in figure 1 could be found in the facts that some centers were clustered (too close to each other).

In figure 5 the Gershgorin circles and eigenvalues for MQ ($\beta = 1.5$) and MQ ($\beta = 0.5$) are presented. Gershgorin theorem states that each eigenvalue λ of the matrix $\mathbf{A}$ satisfies at least one of the following inequalities $|\lambda - \mathbf{a_{kk}}| \leq \mathbf{r_k}$, where $\mathbf{r_k}$ is the sum of all off-diagonal entries in row $\mathbf{k}$ of the matrix $|\mathbf{A}|$.
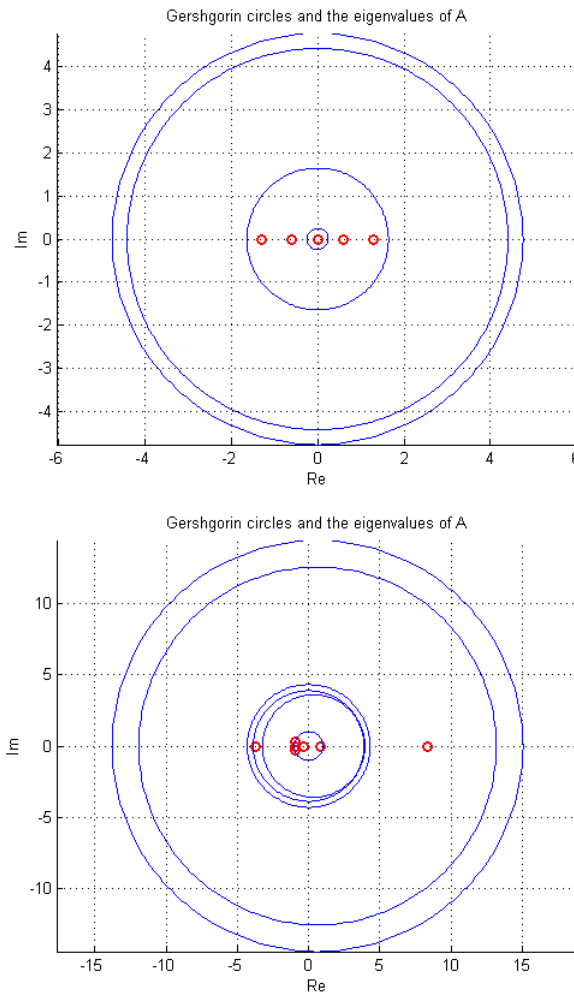

Figure 5: MQ ($\beta = 1.5$) and MQ ($\beta = 0.5$)

The eigenvalues of Kansa's matrix are usually real since matrix is positive

13

definite. The function of matrix is determined with the function of the eigenvalues. Therefore, the effect of the matrix on time dependence problem is declared with eigenvalues of Kansa's matrix. Comparison of Gershgorin circles and the eigenvalues also shows that MQ ($\beta = 1.5$) gives better results than MQ ($\beta = 0.5$). At the same time it is being observed that at the same conditions as above the distribution of eigenvalues are denser at the x axes. Respectively, the eigenvalues lie inside certain maximal disk. Maximal disk has the sum of row elements with mininal radious.

Gerschgorin theorem simplifies and optimizes the calculation of eingevalus of a matrix, which can, otherwise, be quit time consuming work. The very task is limited to summation of elements in a particular row, which gives the length of an interval on which the appropriated eingenvalue lies; position of that interval (or all n-of them) is determined with its centre point and calculated from the diagonal element in row of an approximation matrix.

A space part matrix (approximation matrix) that governs time part of an algorithm can be viewed as a function of a matrix. Function of a matrix can be easily evaluated as function of its spectra, therefore its eingenvalues. This fact makes the task of how approximation matrix works on time loop much easier. It can be plausibly said that for numerical calculation only spectra of approximation matrix must be known explicitly. Geometrically eingenvalues are distributed on real axis along some maximal interval. Intervals, on which eingenvalues are positioned, can be studied for their geometrical properties. They are all concentric and dense. Eigenvalues are all real therefore distributed on real axis. The spectra of a matrix is the very data with which, call it geometric solution, we can see the behaviour of loop, converging goodly or badly. A result known as the Georshgorin theorem is of great benefit for easy derivation of approximate of eingenvalues.

Comparison of positions of the moving boundary calculated with MQ ($\beta = 0.5$) and Integral MQ scheme (Figure 1 and Figure 4) shows that Integral MQ scheme determine better the position of the interfaces than MQ ($\beta = 0.5$). It is known that the integration is a smoothing operation.

Comparison of results calculated with MQ ($\beta = 1.5$) (Figure 2 and Figure 3) also shows that the fulfilment of the equation is better in the interior points (Figure 3) than in the boundary points (Figure 2). The reason could be in using the asymmetric RBF collocation method. Because we want to achieve high accuracy, the resultant system of RBF–PDE problem usually becomes badly conditioned. The solution can be improved by using an affine space decompositon [16] that decouples the influence between the interior and boundary collocations.

It is being also observed that we had better fulfilment of the equation at

collocations points (e.g. upper picture of Figure 2) than at other points (e.g. lower picture of Figure 2). Several different strategies [17] have been somewhat successful in reducing the ill–conditioning problem when using RBF methods in PDE problems. The strategies include: variable shape parameters, domain decomposition, preconditioning the interpolation matrix, and optimizing the center locations.

9   Conclusions

This study presents modelling of moving boundary value problems using a radial basis functions method (MQ, integral MQ). Simulations show that MQ ($\beta = 1.5$) and integral MQ scheme give good results. In this case the method of evaluation was verified by comparing results with the analytical solutions.

We explore the residual error from the equation as an indicator which provides a road map to the optimal selection of the shape parameter value.

In that case of calculating the Stefan's problems we can conclude that the radial basis function methods could be an appropriate alternative to the analytic method due to its simpler implementation.

The choice of basis function is flexible feature of RBF methods. Basis functions may have global or compact support and may have varying degrees of smoothness. The results show that the exponent β need not to be restricted to $\beta = (2m - 1)/2$, $m = 0, 1, 2, 3$, etc.

The Gershgorin circle theorem could be useful tool for choosing an appropriate RBFs. For each value of shape parameter, eigenvalues and their distribution can be studied, therefore obtaining knowledge concerning properties of an approximation matrix and their role being played in finding better approximation of computed data to solution of equation.

The solutions can be improved by using an affine space decompositon that decouples the influence between the interior and boundary collocations.

In our future work we employ a Lagrangian-Eulerian approach to track the movement of the moving boundary and transform the problem to a time-independent domain.

10 Acknowledgements

References

1. Crank, J. (1984). *Free and moving boundary problems*, Clarendon Press, Oxford.

2. Atluri, S. N. and Shen, S. (2002). *The Meshless Local Petrov–Galerkin Method*, Tech Science Press, Encino, CA.

3. Li, G. and Atluri, S. N.(2002). Boundary cloud method: a combined scattered point/boundary integral approach for boundary–only analysis, *Computer. Methods Appl. Engrg.*, Vol. 191, pp. 2337–2370.

4. Kansa, E. J. (1990). Multiquadrics–A scattered data approximation scheme with applications to computational fluid dynamics-I. Surface approximations and partial derivative estimates, *Computers Math. Applic.*, Vol. 19, No. 8–9, pp. 127–145.

5. Kansa, E. J. (1990). Multiquadrics–A scattered data approximation scheme with applications to computational fluid dynamics-II. Solutions to parabolic, hyperbolic and elliptic partial differential equations, *Computers Math. Applic.*, Vol. 19, No. 8–9, pp. 147–161.

6. Hardy, R. L. (1971). Multiquadric equation of topography and other irregular surfaces, *J. Geophys. Res.*, Vol. 176, pp. 1905–1915.

7. Vrankar, L., Turk, G. and Runovc, F. (2004). Modelling of Radionuclide Migration through the Geosphere with Radial Basis Function Method and Geostatistics, *Journal of the Chinese Institute of Engineers.*, Vol. 27, No. 4, pp. 455–462.

8. Vrankar, L., Turk, G. and Runovc, F. (2004). Combining the Radial Basis Function Eulerian and Lagrangian Schemes with Geostatistics for modelling of Radionuclide Migration Through the Geosphere, *Comput. Math. Appl.*, Vol. 48, No. 10–11, pp. 1517-1529.

9. Buhmann, M. D. (2003). *Radial basis functions: theory and implementation, volume 12 of Cambridge Monographs on applied and Computational Mathematics*, Cambridge University Press, Cambridge.

10. Iske, A. (1994), *Charakterisierung bedingt positiv definiter Funktionen für multivariate Interpolationsmethoden mit radialen Basisfunktionen.* Thesis, University Göttingen.

11. Carlson, R. E. and Foley, T. A. (1991). The parameter r^2 in multiqudric interpolation, *Comput. Math. Appl.*, Vol. 21(9), pp. 29-42.

12. Rippa, S (1999). An algorithm for selecting a good parameter c in radial basis function interpolation, *Advances in Computational Mathematics.*, Vol. 11, pp. 193-210.

13. Javierre, E., Vuik, C., Vermolen, F. J. and van der Zwaag, S. (2005). A comparison of numerical models for one–dimensional Stefan problems, *Reports of the Delft Institute of Applied Mathematics*, Netherlands.

14. Hill, J. M. (1987). *One–dimensional Stefan problems: an introduction*, Longman Scientific and Technical, Harlow.

15. Mai–Duy, N. and Tran–Cong, T. (2001). *Numerical solution of differential equations using multiquadric radial basis function networks*, Approx. Neural Networks, Vol. 14, pp. 185–199.

16. Ling, L. and Hon, Y. C. (2005). Improved numerical solver for Kansa's method based on affine space decomposition, *Eng. Anal Bndy. Elem.*, Vol. 29, pp. 1077–1085.

17. Kansa, E. J. and Hon, Y. C. (2000). Circumventing the ill–conditioning problem with multiquadric radial basis functions: Applications to elliptic partial differential equations, *Computers Math. Applic.*, Vol. 39, No. 7–8, pp. 123–137.